

Sparsity-Inducing Categorical Prior Improves Robustness of the Information Bottleneck

Anirban Samaddar¹

Sandeep Madireddy²

Prasanna Balaprakash²

¹Department of Statistics and Probability, Michigan State University, East Lansing, Michigan, USA

²Mathematics and Computer Science Division, Argonne National Laboratory, Lemont, Illinois, USA

Abstract

The information bottleneck framework provides a systematic approach to learn representations that compress nuisance information in inputs and extract semantically meaningful information about the predictions. However, the choice of the prior distribution that fix the dimensionality across all the data can restrict the flexibility of this approach to learn robust representations. We present a novel sparsity-inducing spike-slab prior that uses sparsity as a mechanism to provide flexibility that allows each data point to learn its own dimension distribution. In addition, it provides a mechanism to learn a joint distribution of the latent variable and the sparsity. Thus, unlike other approaches, it can account for the full uncertainty in the latent space. Through a series of experiments using in-distribution and out-of-distribution learning scenarios on the MNIST and Fashion-MNIST data we show that the proposed approach improves the accuracy and robustness compared with the traditional fixed-dimensional priors as well as other sparsity-induction mechanisms proposed in the literature.

1 INTRODUCTION

The information bottleneck (IB) (Tishby et al. [2000]) is a deep latent variable model that poses representation compression as a constrained optimization problem to find representations Z that are maximally informative about the outputs Y while being maximally compressive about the inputs X , by means of a loss function expressed using a mutual information (MI) metric and a Lagrangian formulation of the constrained optimization: $\mathcal{L}_{IB} = \text{MI}(X; Z) - \beta \text{MI}(Z; Y)$. Here $\text{MI}(X; Z)$ is the MI that reflects how much the representation compresses X , and $\text{MI}(Z; Y)$ reflects how much information the representation has kept from Y .

It is a standard practice to use parametric priors such

as a mean field Gaussian prior for the latent variable Z , as seen with most latent-variable models in the literature (Tomczak [2022]). In general, however, a major limitation of these priors is the requirement to preselect a latent space complexity for all data, which can be very restrictive and lead to models that are less robust. Sparsity, when used as a mechanism to choose the complexity of the model in a flexible and data-driven fashion, has the potential to improve the robustness of machine learning systems without loss in accuracy, especially when dealing with high-dimensional data (Ahuja et al. [2021]).

Sparsity has been considered in the context of latent variable models by a handful of works, but mostly in the context of unsupervised learning. Notable works include the sparse Dirichlet variational autoencoder (sDVAE) (Burkhardt and Kramer [2019]), epitome VAEs (eVAE) (Yeung et al. [2017]), variational sparse coding (VSC) (Tonolini et al. [2020]), and Intel-VAE (Miao et al. [2022]). Most of these approaches do not take into account the uncertainty involved in introducing sparsity and treat this as a deterministic selection problem. Ignoring the uncertainty in the selection can lead to loss of robustness in inference and prediction. Although the application of the Indian buffet process (IBP) in VAE (Singh et al. [2017], Griffiths and Ghahramani [2011]) provided a way to define distribution over the selection parameters inducing sparsity, since it was developed primarily for topic models, the selection of the latent dimension occurs in IBP by setting some of the latent variables zero for all observations. This might not be ideal for dimensionality reduction or representation learning in complex supervised learning tasks where each data point may exhibit a different number of latent features, in which case the IBP model can be oversimplified.

While all these approaches have been proposed for the unsupervised learning, we are interested in the supervised learning scenario introduced with the IB approach, which poses a different set of challenges because the sparsity has to cater to accurately predicting Y . Only one recent work (Kim et al. [2021]) that we know of has considered sparsity in the latent variables of the IB model, but here the latent

variable is assumed to be deterministic, and the sparsity applied indirectly by weighting each dimension using a Bernoulli distribution, where zero weight is equivalent to sparsifying.

In this work we introduce a novel sparsity-inducing Bayesian spike-slab prior for supervised learning in the IB framework. In this approach, the sparsity in the latent variables of the IB model is modeled stochastically through a categorical distribution, and thus the joint distribution of them (latent variable and the sparsity) is learned with this categorical prior IB (CP-IB) model through a Bayesian inference. Learning the joint distribution provides the flexibility to systematically learn data-specific latent dimension complexity, account for the full uncertainty, and thus enable them to learn parsimonious and robust representations.

We also derive variational lower bounds for the proposed CP-IB model and, using a series of experiments in the in-distribution and out-of-distribution scenarios, show the improvement of the accuracy and robustness of our proposed approach when compared with the vanilla IB models with fixed Gaussian priors and other sparsity-inducing strategies proposed in the literature.

2 RELATED WORK

Previous works in the IB and VAE literature have looked at different sparsity-inducing mechanisms in the latent space in supervised and unsupervised settings. Burkhardt and Kramer [2019] propose a sparse Dirichlet variational autoencoder (sDVAE) that assumes a degenerate Dirichlet distribution over the latent variable. They introduce sparsity on the concentration parameter of the Dirichlet distribution via a deterministic neural network. Epitome VAE (eVAE) by Yeung et al. [2017] imposes sparsity via epitomes that select adjacent coordinates of the mean-field Gaussian latent vector and mask the others before feeding to the decoder. The authors propose to train a deterministic epitome selector to select from all possible epitomes. Similar to eVAE, the variational sparse coding (VSC) proposed in Tonolini et al. [2020] introduces sparsity through a deterministic classifier. In this case the classifier outputs an index from a set of pseudo inputs that define the prior for the latent variable. In more recent work, Intel-VAE (Miao et al. [2022]) introduces sparsity via a dimension selector (DS) network on top of the Gaussian encoder layer in standard VAEs. The output of DS is multiplied with the Gaussian encoder to induce sparsity and then is fed to the decoder. Intel-VAE has empirically shown improvement over VSC in unsupervised learning tasks such as image generation.

In the IB literature we find the aspect of sparsity in the latent space seldom explored. To our knowledge, Drop-Bottleneck (Drop-B) by Kim et al. [2021] is the only work that attempts this problem. In Drop-B, a neural network extracts features from the data; then a Bernoulli random variable stochastically drops certain features before passing it to the decoder. The probabilities of the Bernoulli distribu-

tion are assumed as global parameters and are trained with other parameters of the model.

In this paper we assume the stochasticity of both latent variable and sparsity. In this aspect we differ from most of the existing works in this direction. Our method, CP-IB, by learning the joint distribution of latent variable and sparsity, tries to fully account for the uncertainty in the latent space. The Indian buffet process (Singh et al. [2017]) is also a parallel way to achieve a similar objective. IBP induces distribution over infinite-dimensional sparse matrices where each element of the matrix is an independent Bernoulli random variable. As in the Drop-B, the Bernoulli probabilities in IBP are global parameters that further comes from a Beta distribution. Therefore, the sparsity induced by IBP is global and can make coordinates of the latent variable zero for all the data points. However, our approach lifts this restriction by learning the distribution of sparsity for each data point.

In Table 1 we summarize these different approaches by the types, stochastic (S) or deterministic (D), of the latent variable and the sparsity. The table shows that very few works incorporate stochasticity in the latent variable as well as the sparsity-inducing mechanism.

Approach	Latent Variable	Sparsity
sDVAE	S	D
eVAE	S	D
VSC	S	D
Intel-VAE	S	D
Drop-B	D	S
IBP	S	S
CP-IB	S	S

Table 1: Latent-variable models with different sparsity induction strategies, where D=Deterministic and S=Stochastic.

3 INFORMATION BOTTLENECK WITH SPARSITY-INDUCING CATEGORICAL PRIOR

3.1 INFORMATION BOTTLENECK: PRELIMINARIES

Considering a joint distribution $P(X, Y)$ of the input variable X and the corresponding target variable Y , the information bottleneck principle aims to find a (low-dimensional) latent encoding Z by maximizing the prediction accuracy, formulated in terms of the mutual information $MI(Z; Y)$, given a constraint on the compressing the latent encoding, formulated in terms of the mutual information $MI(X; Z)$. This can be cast as a constrained optimization problem:

$$\begin{aligned} \max_Z & MI(Z; Y) \\ \text{s.t.} & MI(X; Z) \leq C, \end{aligned} \quad (1)$$

where C can be interpreted as the compression rate or the minimal number of bits needed to describe the input data. The mutual information is obtained through a multidimensional integral that depends on the joint distribution and marginal distribution of random variables given by

$\int_{\mathcal{Z}} \int_{\mathcal{X}} P_{\theta}(x, z) \log \left(\frac{P_{\theta}(x, z)}{P(x)P(z)} \right) dx dz$, where $P_{\theta}(x, z) := P_{\theta}(z|x)P(x)$; a similar expression for $MI(Z; Y)$ needs $P_{\theta}(y, z) := \int P_{\theta}(z|x)P(x, y)dx$. The integral presented for calculating the MI is in general computationally intractable for large data.

Thus, in practice, the Lagrangian relaxation of the constrained optimization problem is adopted Tishby and Zaslavsky [2015]:

$$\mathcal{L}_{IB}(Z) = MI(Z; Y) - \beta * MI(X; Z), \quad (2)$$

where β is a Lagrange multiplier that enforces the constraint $MI(X; Z) \leq C$ such that a latent encoding Z that is maximally expressive about Y while being maximally compressive about X is desired. In other words, $MI(X; Z)$ is the mutual information that reflects how much the representation (Z) compresses X , and $MI(Z; Y)$ reflects how much information the representation has been kept from Y . Several approaches have been proposed in the literature to approximate the mutual information $MI(X; Z)$, ranging from parametric bounds defined by the variational lower bounds (Alemi et al. [2016]) to the nonparametric (kernel density estimate-based) bounds (Kolchinsky et al. [2019]) and adversarial f-divergences Zhai and Zhang [2021]. In this research we focus primarily on the variational lower bounds-based approximation.

Role of Prior Distribution and the Stochasticity of the Latent Variable In the IB formulation presented above, the latent variable is assumed to be stochastic, and hence the posterior distribution of it is learned by using Bayesian inference. In Alemi et al. [2016], the variational lower bound of $\mathcal{L}_{IB}(Z)$ is given as

$$\mathcal{L}_{VIB}(Z) = \mathbb{E}_{X, Y} \left[\mathbb{E}_{Z|X} \log q(Y|Z) - \beta * D_{KL}(q(Z|X)||q(Z)) \right]. \quad (3)$$

In the loss equation (3), the prior $q(z)$ serves as a penalty to the variational encoder $q(z|x)$ and $q(y|z)$ is the decoder that is the variational approximation to $p(y|z)$. Alemi et al. [2016] choose the encoder family and the prior to be a fixed K -dimensional isotropic multivariate Gaussian distribution ($N(0_K, I_{K \times K})$). This choice is motivated by the simplicity and efficiency of inference using differentiable reparameterization of the Gaussian random variable Z in terms of its mean and sigma. For complex datasets, however, this can be restrictive since the same dimensionality is imposed on all the data and hence can prohibit the latent space from learning robust features (Miao et al. [2022]).

We describe a new family of sparsity-inducing priors that allow stochastic exploration of different dimensional latent spaces. For the proposed variational family we derive the variational lower bound that consists of discrete and continuous variables, and we show that simple reparameterization

steps can be taken to draw samples efficiently from the encoder for inference and prediction.

3.2 SPARSITY-INDUCING CATEGORICAL PRIOR

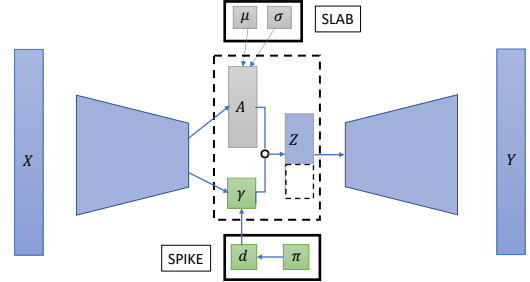


Figure 1: Schematic of the categorical process information bottleneck (CP-IB) model. The inputs are passed through the encoder layer to estimate the feature allocation vector A , while simultaneously using a categorical process to sample the number of active dimensions d of A for given data that selects the complexity of latent variable Z . The obtained Z is then fed to the decoder to predict the supervised learning responses.

A key aspect of the IB model, and latent variable models in general, is the dimension of Z . Fixing a very low dimension of Z can impose a limitation on the capacity of the model, while a very large Z can lead to learning a lot more nuisance information that can be detrimental for model robustness and generalizability. We formulate a data-driven approach to learn the distribution of the dimensionality Z through the design of sparsity-inducing prior.

Let $\{X_n, Y_n\}_{n=1}^N$ be N data points, and let the latent variable $Z_n = (Z_{n,1}, Z_{n,2}, \dots, Z_{n,K})'$, where K is the latent dimensionality. The idea is that we will fix K to be large a priori and make the prior assumption that $k < K$ columns of Z_n are zero and hence do not contribute in predicting Y_n . Therefore, the prior distribution of Z_n can be specified as follows.

$$Z_{n,k} | \gamma_{n,k} \stackrel{ind}{\sim} (1 - \gamma_{n,k}) \mathbb{1}(Z_{n,k} = 0) + \gamma_{n,k} \mathcal{N}(\mu_{n,k}, \sigma_{n,k}^2)$$

OR

$$Z_n = A_n \circ \gamma_n \quad (4)$$

$$A_n \sim \mathcal{N}(\mu_n, \Sigma_n) \quad (5)$$

$$\gamma_{n,k} | d_n = \mathbb{1}(k \leq d_n) \quad (6)$$

$$d_n \sim \text{Categorical}(\pi_n) \quad (7)$$

This prior is a variation of the spike-slab family (George and McCulloch [1993]) where the sparsity-inducing parameters follow a categorical distribution. The latent variable Z_n is an elementwise product between the feature allocation vector A_n and a sparsity-inducing vector γ_n . The K -dimensional latent A_n is assumed to follow a K -dimensional Gaussian distribution with mean vector μ_n and diagonal covariance matrix Σ_n with the variance vector σ_n^2 . Note that γ_n is a vector whose first d_n coordinates are 1s and rest are 0s, and hence $A_n \circ \gamma_n$, with the result that the first

d_n coordinates of Z_n are nonzero and the rest are 0. Hence, as we sample d_n , we consider the different dimensionality of the latent space; d_n follows a categorical distribution over K categories with π_n as the vector of categorical probabilities whose elements $\pi_{n,k}$ denote the prior probability of k th dimension for data n . In Fig. 1 we present the flow of the model from the input X to the output Y through the latent encoding layer.

3.3 DERIVATION OF THE VARIATIONAL BOUND

The variable d_n augments Z_n for the latent space characterization. With a Markov chain assumption, $Y \leftrightarrow X \leftrightarrow (Z, d)$, the latent variable distribution factorization as $p(Z, d) = \prod_{n=1}^N p(Z_n|d_n)p(d_n)$, and the same family with the same factorization of the variational posterior $q(Z_n, d_n|X_{1:n})$ as the prior. We derive the variational lower bound of the IB Lagrangian as follows.

$$\begin{aligned} \mathcal{L}_{\text{CP-IB}}(Z) &\geq \mathcal{L}_{\text{VIB}}(Z) \\ &= \mathbb{E}_{X,Y} \left[\mathbb{E}_{Z|X} \log q(Y|Z) \right. \\ &\quad \left. - \beta \text{D}_{\text{KL}}(q(Z, d|X) || q(Z, d)) \right] \end{aligned}$$

Note that we have introduced the random variable d along with Z in the density function of the second KL-term. This is because the KL-divergence between $q(Z|X)$ and $q(Z)$ is intractable. The last equality holds since $d = \sum_{k=1}^K \mathbb{1}(Z_k \neq 0)$ is a deterministic function of Z , and we can write the density $q(z, d) = q(z)\delta_{d_z}(d)$, where $\delta_a(d)$ is the Dirac delta function at a . Therefore we have the following.

$$\begin{aligned} &\text{D}_{\text{KL}}(q(Z, d|X) || q(Z, d)) \\ &= \mathbb{E}_{Z,d|X} \log \frac{q(Z|X)\delta_{d_z}(d)}{q(Z)\delta_{d_z}(d)} \\ &= \mathbb{E}_{Z|X} \mathbb{E}_{d|Z} \log \frac{q(Z|X)\delta_{d_z}(d)}{q(Z)\delta_{d_z}(d)} \\ &= \mathbb{E}_{Z|X} \log \frac{q(Z|X)}{q(Z)} = \text{D}_{\text{KL}}(q(Z|X) || q(Z)) \end{aligned}$$

We now replace the $\mathbb{E}_{X,Y}$ with the empirical version.

$$\begin{aligned} \mathcal{L}_{\text{CP-IB}}(Z) &\hat{=} \frac{1}{N} \sum_{n=1}^N \left[\mathbb{E}_{Z_n|X_n} [\log q(Y_n|Z_n)] \right. \\ &\quad \left. - \beta \text{KL}(q(Z_n, d_n|X_n) || q(Z_n, d_n)) \right] \\ &= \frac{1}{N} \sum_{n=1}^N \left[\mathbb{E}_{d_n|X_n} \mathbb{E}_{Z_n|X_n, d_n} [\log q(Y_n|Z_n)] \right. \\ &\quad \left. - \beta \left[\mathbb{E}_{d_n|X_n} [\text{KL}(q(Z_n|X_n, d_n) || q(Z_n|d_n))] \right. \right. \\ &\quad \left. \left. + \text{KL}(q(d_n|X_n) || q(d_n)) \right] \right] \end{aligned}$$

We analyze the three terms in the above decomposition as follows.

$$\begin{aligned} (i) \quad &\mathbb{E}_{d_n|X_n} \mathbb{E}_{Z_n|X_n, d_n} [\log q(Y_n|Z_n)] \\ &= \sum_{k=1}^K \mathbb{E}_{Z_n|X_n, d_n=k} [\log q(Y_n|Z_n, d_n = k)] \pi_k(X_n) \end{aligned}$$

This term is a weighted average of the negative cross-entropy losses from models with increasing dimension of latent space, where the weights are the posterior probabilities of the dimension encoder. Hence, *maximizing this term implies putting large weights on the dimensions of the latent space where Z becomes more expressive*. While training, this term can be computed by Monte Carlo approximation, that is, $(i) \hat{=} \frac{1}{J} \sum_{j=1}^J \log q(Y_n|Z_n = Z_n^{(j)}, d_n = d_n^{(j)})$, where we draw J randomly drawn samples from $q(Z_n, d_n|X_n)$.

$$\begin{aligned} (ii) \quad &\mathbb{E}_{d_n|X_n} [\text{D}_{\text{KL}}(q(Z_n|X_n, d_n) || q(Z_n|d_n))] \\ &= \sum_{k=1}^K \text{D}_{\text{KL}}(q(Z_n|X_n, d_n = k) || q(Z_n|d_n = k)) \pi_k(X_n) \end{aligned}$$

Note that $q(z_n|d_n) = q(z_n|\gamma_n) = \mathcal{N}(z_n; \tilde{\mu}_n, \tilde{\Sigma}_n)$, where $\tilde{\mu}_n = \mu_n \circ \gamma_n$ and $\tilde{\Sigma}_n$ is diagonal with entries $\tilde{\sigma}_n^2 = \sigma_n^2 \circ \gamma_n$. When $k < K$, this density does not exist w.r.t the Lebesgue measure in \mathbb{R}^K . However, we can still define a density w.r.t the Lebesgue measure restricted to \mathbb{R}^k (see Chapter 8 in Rao [1973]), and it is the k -dimensional multivariate normal density with mean $\mu_{n, -\overline{K-k}} = (\mu_{n,1}, \dots, \mu_{n,k})'$ and diagonal covariance matrix $\Sigma_{n, -\overline{K-k}}$ with diagonal entries $\sigma_{n, -\overline{K-k}}^2 = (\sigma_{1,n}^2, \dots, \sigma_{n,k}^2)'$. Denoting $\mu_{n,-0} = \mu_n$, we have the following.

$$\begin{aligned} (ii) \quad &\mathbb{E}_{d_n|X_n} [\text{D}_{\text{KL}}(q(Z_n|X_n, d_n) || q(Z_n|d_n))] \\ &= \sum_{k=1}^K \text{D}_{\text{KL}} \left(\mathcal{N}(\mu_{n, -\overline{K-k}}(x_i), \Sigma_{n, -\overline{K-k}}(x_i)) \right. \\ &\quad \left. || \mathcal{N}(\mu_{n, -\overline{K-k}}, \Sigma_{n, -\overline{K-k}}) \right) \pi_k(x_i) \\ &= \sum_{k=1}^K \sum_{\ell=1}^k \text{D}_{\text{KL}} \left(\mathcal{N}(\mu_{n,\ell}(x_i), \sigma_{n,\ell}^2(x_i)) \right. \\ &\quad \left. || \mathcal{N}(\mu_{n,\ell}, \sigma_{n,\ell}^2) \right) \pi_k(x_i) \end{aligned}$$

The last equality is due to the fact that KL-divergence of multivariate Gaussian densities whose covariances are diagonal can be written as a sum of coordinate-wise KL-divergences. Since KL-divergence is always non-negative, *minimizing the above expression implies putting more probability to the smaller-dimensional latent space models since the second summation term is expected to grow with dimension k* .

$$(iii) \quad \text{D}_{\text{KL}}(q(d_n|X_n) || q(d_n)) = \sum_{k=1}^K \log \frac{\pi_{n,k}(X_n)}{\pi_{n,k}}$$

Minimizing this term forces the learned probabilities to be close to the prior. Note that we are learning these probabilities for each data point (as $\pi_{n,k}(X_n)$ is indexed by n). In this respect we differ from most of the stochastic sparsity-inducing approaches such as the Drop-IB (Kim et al. [2021]) and the IBP (Singh et al. [2017]). In those approaches, the sparsity is induced from a probability distribution with global parameterization and not learned for each data point.

Modeling Choices for the CP-IB Components: Since $Z_n = A_n \circ \gamma_n$, we are required to fix the priors for (A_n, γ_n) or (A_n, d_n) . We chose K -dimensional spherical Gaussian $\mathcal{N}(0, I_K)$ as the prior for the latent variable A_n . For d_n , we assume that the k th categorical probability is from the compound distribution of a beta-binomial model, also known as the Poly urn model Mahmoud [2008]. Therefore,

$$\pi_n = \mathbb{P}(d_n = k) = \binom{K-1}{k-1} \frac{B(a_n + k - 1, b_n + p - k)}{B(a_n, b_n)}. \quad (8)$$

For simplicity we fix the prior value to be constant across data points, that is, $(a_n, b_n) = (a, b)$. The key advantage of this choice is that we can write the probability as a differentiable function of the two shape parameters (a_n, b_n) . Therefore, we can assume the same distribution for the encoder; and instead of learning K probabilities $\pi_{n,k}(X_n)$ we can learn $(a_n(X_n), b_n(X_n))$, which significantly reduces the dimensionality of the parameter space. However, learning $\pi_{n,k}(X_n)$ provides more flexibility because the shape of the probabilities is not constrained, whereas learning $\pi_{n,k}(X_n)$ through $(a_n(X_n), b_n(X_n))$ constrains the shape of the probabilities, which is dependent on $a_n(X_n)$ and $b_n(X_n)$. In our experiments we tried both approaches and found that learning $(a_n(X_n), b_n(X_n))$ produce better results.

4 EXPERIMENTAL RESULTS

In this section we present experimental results comparing the performance of VIB with the proposed sparsity-inducing prior approach CP-IB with other sparsity-inducing strategies proposed in the literature for latent variable models by adapting them in the context of information bottleneck. In addition, we compare our model with the baseline VIB approach, where a mean-field Gaussian distribution is used as a prior and the latent dimension is fixed to a single value across all data.

A key requirement for any machine learning model is its ability to *generalize*. Generalization refers to reducing the gap in performance of the model between training and testing scenarios. Both training and testing scenarios could be *in-distribution* or *out-of-distribution*. In-distribution scenarios are the most frequently studied learning scenarios, but generalization to out-of-distribution scenarios will greatly increase the robustness of the model. Out-of-distribution scenarios may arise because of nonstationarity in temporally acquired data (or hidden factors), whether the data shift

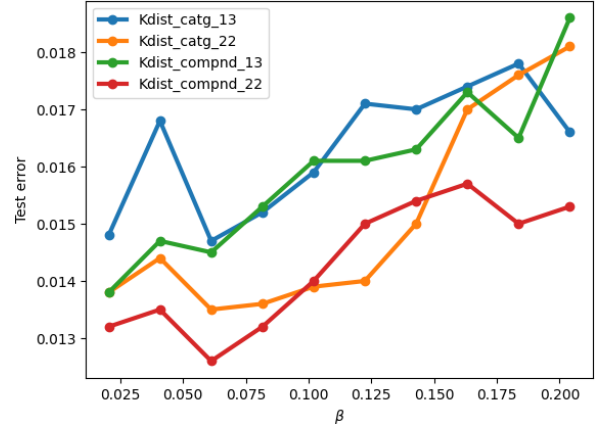


Figure 2: Plot of test error vs β . It shows that compound distribution prior with $(a, b) = (2, 2)$ produces the lowest test error across β .

is gradual or abrupt, such as rotation or noise corruptions. Adversarial perturbations to the input data also result in out-of-distribution scenarios, albeit with special properties (Tramèr et al. [2020]).

We evaluate the CP-IB model for in-distribution prediction accuracy in a supervised classification scenario using the MNIST and Fashion-MNIST data. Furthermore, we assess the robustness of CP-IB in the out-of-distribution scenarios, specifically with rotation, white-box attacks with noise corruptions, and black-box adversarial attacks.

4.1 IN-DISTRIBUTION

For the proposed CP-IB model we need to select the neural architecture to be used for the slab distribution encoder as well as the dimension encoder that learns either the categorical probabilities or the compound distribution parameters. For MNIST, we follow Rodríguez Gálvez et al. [2020] and use an MLP encoder with three fully connected layers, the first two of 800 dimensions and ReLu activation and the last one of $2K$ dimensions. The decoder consists of two fully connected layers, the first of which has 800 dimensions and the second predicts the softmax class probabilities in the last layer. The neural architecture for the dimension encoder is the same as for the encoder until the final layer. The final layer in the dimension encoder has K nodes with a softmax function for learning the probabilities and 2 nodes with a softplus function for learning the compound parameters. For Fashion-MNIST, following Rodríguez Gálvez et al. [2020], we adopt a CNN encoder and an MLP decoder. The encoder is a 2-layer CNN with 32 filters on the first layer and 128 on the second layer. In both layers we used kernels of size 5 and stride 2. The CNN layers are followed by two fully connected layer—the first one of dimension 128 and the second one of $2K$ dimensions—and ReLu activation between them. The decoder in this case is an MLP with the same architecture as for the MNIST. Here also we use the same *dimension encoder* architecture as the encoder until the final layer. The final layer is the same as for MNIST.

For comparison with other sparsity-inducing approaches,

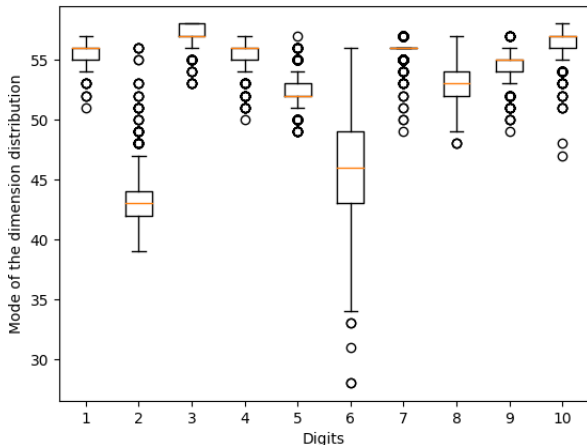


Figure 3: Plot of dimension distribution modes aggregated for each class. It shows that sparsity-inducing prior (compound distribution prior with $(a, b) = (2, 2)$) provides flexibility to learn the data-specific latent dimension distribution, in contrast to fixing to a single value.

we choose the two most recent works: the Drop-B model (Kim et al. [2021]) and the Intel-VAE (Miao et al. [2022]). The Drop-B implementation requires a feature extractor. For both MNIST and F-MNIST, we choose the same architecture for the feature extractor as the encoder of CP-IB until the final layer, which has K dimensions. We assume the same decoder architecture for Drop-B as for CP-IB. Additionally for Drop-B, the K Bernoulli probabilities are trained with the other parameters in the model. For Intel-VAE, the encoder and decoder architectures are the same as in CP-IB for MNIST and F-MNIST. In addition, this model requires a dimension selector (DS) network. Following the experiments Miao et al. [2022], we select three fully connected layers for the DS network with ReLU activations in between, where the first two layers have dimension 10 and the last layer has dimension K . In this section these two approaches are called Drop-VIB and Intel-VIB. We fix K (i.e., the prior assumption on dimensionality) to be 100 for all methods.

The workflow of CP-IB overlaps with the standard VIB when we are encoding the mean and sigma of the latent variable. Additionally the CP-IB encodes the categorical probabilities and then draws samples from a categorical distribution. Unlike the reparameterization trick (Kingma and Welling [2014]) for the Gaussian variables, there does not exist a differentiable transformation from categorical probabilities to the samples. Therefore, we use the Gumbel-softmax approximation (Maddison et al. [2017], Jang et al. [2017]) to draw the categorical samples. We apply the transformation in (6) to the categorical samples and take the elementwise product with the Gaussian samples before passing it to the decoder. Following Kolchinsky et al. [2019], we square the compression term for the image classification experiments. Taking a convex transformation of the compression term makes the solution of the IB Lagrangian identifiable (Rodríguez Gálvez et al. [2020]).

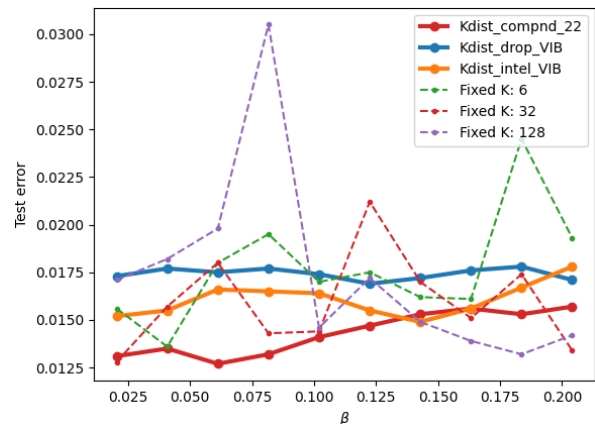


Figure 4: Plot of test error vs β comparison with vanilla VIB models with fixed latent dimension of 6, 32, 128 and drop-VIB and intel-VIB. It shows that compound distribution prior with $(a, b) = (2, 2)$ produces the lowest test error across all the models.

To evaluate the effect of the prior distribution, we evaluate at two different cases, with $(a, b) = (1, 3)$ and $(2, 2)$ for both the categorical and compound distribution strategies. Fig. S2 shows the prior probabilities of dimensions for both choices. We can see that the choice $(a, b) = (1, 3)$ puts more probability mass on the lower dimensions and it gradually decays with dimension, whereas $(a, b) = (2, 2)$ penalizes too high- or too low-dimensional models. Moreover, we evaluate how the accuracy on the test data changes with the β value that was used while training. We find that for MNIST data, the compound distribution prior with $(a, b) = (2, 2)$ performs the best in terms of prediction accuracy across the variation in β , as shown in Fig. 2.

A distinct feature of the proposed approach is the flexibility enabled by the sparsity-inducing prior to learning a data-dependent dimension distribution. To demonstrate that, in Fig. 3 we show a boxplot of posterior modes of dimension distribution across data points, aggregated per digit. We see that, in fact, each digit on average preferred to have a different latent dimension. We further note that the median values depicted by the box plot for digits 2 and 6 are farther away from the medians of rest of the digits.

We observe a slightly different behavior on the F-MNIST data, where we find that the compound $(1, 3)$ prior distribution achieves a lower test error compared with that of the $(2, 2)$ distribution (Fig. S3 (a)). Furthermore, in Fig. S3 (b) the separation between the medians of the dimension distribution modes for each digit is significant, further emphasizing the importance of flexible prior distribution. The test error for F-MNIST data is low for both the compound prior model and the drop VIB for small values of β (Fig. S3 (c)), but the difference between them widens as the β increases. We show in the next section that even though the error is not the lowest for the compound distribution prior compared with the drop VIB, the former is much more robust when evaluated against out-of-distribution scenarios. We evaluate the performance of each model using a

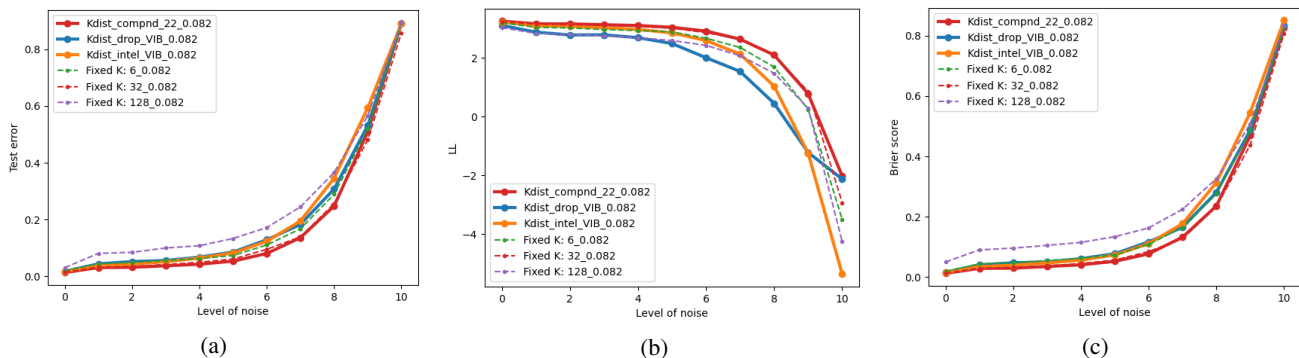


Figure 5: Plot of the test error, the log-likelihood, and the Brier score against the level of noise added to the test dataset. We observe that compound prior distribution with $(a, b) = (2, 2)$ (red solid line) performs best in most of the cases.

single β value. The β value for MNIST is ~ 0.08 and for F-MNIST is ~ 0.06 . The choice of β value is discussed in the supplementary materials (Section 6.1).

4.2 OUT-OF-DISTRIBUTION

We consider three out-of-distribution scenarios to measure the robustness of our approach and compare it with vanilla VIB with fixed latent dimension capacity as well with other sparsity-inducing strategies. The first is a white-box attack, where we systematically introduce shot noise corruptions into the test data following the procedure used in Corrupted-MNIST work of Mu and Gilmer [2019]. The second is the black-box adversarial attack simulated through the project gradient descent (PGD) strategy Madry et al. [2019]. The third is with data generated by applying a rotation transform to the MNIST data, which corresponds to a nonstationarity transform.

4.2.1 White-box attack – Noise corruption

The white-box attack or noise corruption is generated through the addition of shot noise. Following Mu and Gilmer [2019], Poisson noise is generated pixelwise and added to the test images for both MNIST and F-MNIST. The levels of noise along the x-axis of Fig. 5 represent increasing degree of noise added to the test set images. Figure 6 shows the impact of adding increasing levels of noise to a sample test set MNIST image. For our approach and each of the five models that are being compared, we plot the test error, log likelihood, and Brier score as a function of the level of noise to assess the robustness of these approaches. We find that with both MNIST (Fig. 5) and F-MNIST (Fig. S4), for each of these three metrics the compound distribution prior outperforms all the other compared approaches.

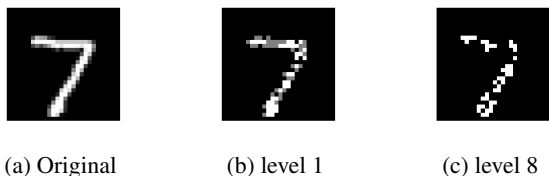


Figure 6: Impact of increasing noise level.

4.2.2 Black-box (adversarial) attack

Multiple approaches have been proposed in the literature to assess the adversarial robustness of a model Tramer et al. [2020]. Among them, perhaps the most commonly adopted approach is to test the accuracy on adversarial examples that are generated by adversarially perturbing the test data. This perturbation is in the same spirit as the noise corruption presented in the preceding section but is designed to be more catastrophic by adopting a black-box attack approach that chooses a gradient direction of the image pixels at some loss and then takes a single step in that direction. The projected gradient descent is an example of such an adversarial attack. Following Alemi et al. [2016], we evaluate the model robustness for the PGD attack with one iteration, and additionally we perform another case with 20 iterations to simulate a stronger attack. We use the L_∞ norm to measure the size of the perturbation, which in this case is a measure of the largest single change in any pixel. The test error as a function of the perturbed L_∞ distance for all six approaches for the MNIST data is shown in Fig. 8. We note that even though the Drop-VIB gives the best robustness at a weaker attack, the CP-IB approach provides the lowest error for the stronger attack. The corresponding results for F-MNIST is shown in Fig. S5.

4.2.3 Rotation

In this scenario we evaluate the models trained on MNIST data with increasingly rotated digits following Ovadia et al. [2019], which simulates the scenario of data that is moderately out of distribution to the data used for training the model. We show the results of the experiments in Fig. 7, where we can see that CP-IB with the compound distribution prior outperforms the rest of the five models in terms of the prediction error, log likelihood, and Brier score, we also note that the performance of the Drop-VIB has the lowest performance in this scenario, which is more apparent in the log-likelihood plot.

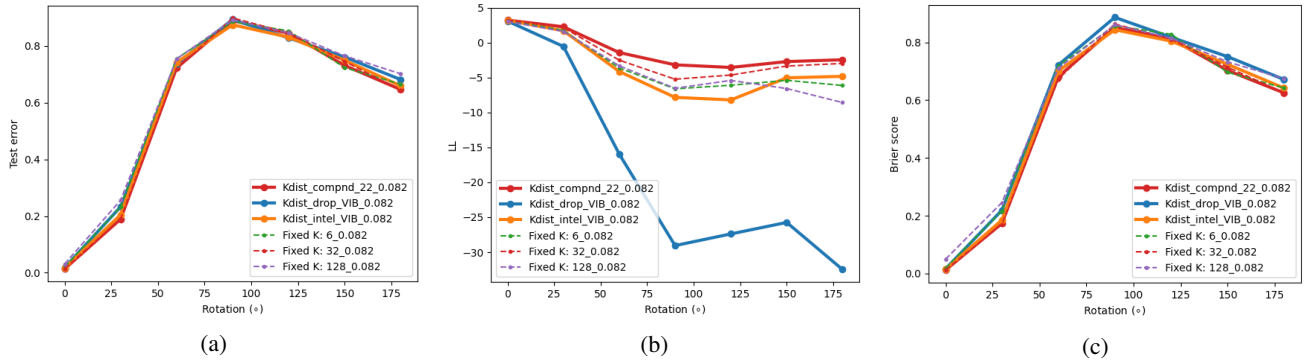


Figure 7: Plot of the test error, the log-likelihood, and the Brier score against rotation in the case of the rotated test dataset. We observe that compound prior distribution with $(a, b) = (2, 2)$ (red solid line) performs best in most of the cases.

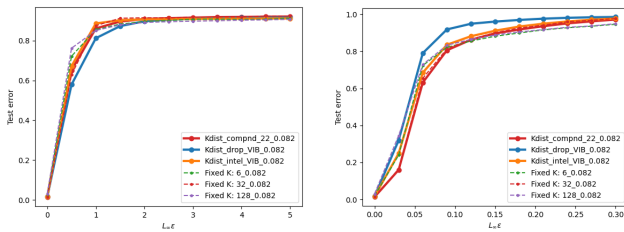


Figure 8: Plot of the test error vs PGD L_∞ attack radius of the models with 1 iteration (left) and 10 iterations (right). It shows that compound distribution prior with $(a, b) = (2, 2)$ produces the lowest test error across models when the attack is strong, while the Drop-VIB gives the lowest error when the number of iterations is one (i.e., weaker attack).

5 CONCLUSIONS

In this work we propose a sparsity-inducing spike-slab prior for Bayesian inference of the stochastic latent variable in the information bottleneck model. This prior introduces sparsity stochastically through the spike distribution defined with a categorical prior, while the slab distribution can be any continuous distribution such as Gaussian distribution. This approach, referred to as CP-IB, learns a joint distribution of the latent variable and the sparsity. Thus, unlike other approaches, it can account for the full uncertainty in the latent space. In addition, we are able to learn the distributions for each data point, thus allowing data the flexibility of choosing their own dimension distribution. Consequently, we find through a series of experiments on MNIST and Fashion-MNIST in both the in-distribution and out-of-distribution scenarios (such as noise corruption, adversarial attacks, and rotation) that our approach obtains better accuracy and robustness compared with the commonly used fixed-dimensional priors as well as using that sparsity-inducing strategies previously proposed in the literature.

As part of future work we will further generalize the categorical prior spike distribution through a nonparametric treatment, explore other approaches to data-driven mutual information estimation to tighten the lower bound, and apply this approach to real-world scientific datasets.

References

- Kartik Ahuja, Ethan Caballero, Dinghui Zhang, Yoshua Bengio, Ioannis Mitliagkas, and Irina Rish. Invariance principle meets information bottleneck for out-of-distribution generalization, 2021.
- Alexander A Alemi, Ian Fischer, Joshua V Dillon, and Kevin Murphy. Deep variational information bottleneck. *arXiv preprint arXiv:1612.00410*, 2016.
- Sophie Burkhardt and Stefan Kramer. Decoupling sparsity and smoothness in the Dirichlet variational autoencoder topic model. *J. Mach. Learn. Res.*, 20(131):1–27, 2019.
- Edward I George and Robert E McCulloch. Variable selection via Gibbs sampling. *Journal of the American Statistical Association*, 88(423):881–889, 1993.
- Thomas L. Griffiths and Zoubin Ghahramani. The Indian buffet process: An introduction and review. *Journal of Machine Learning Research*, 12(32):1185–1224, 2011. URL <http://jmlr.org/papers/v12/griffiths11a.html>.
- Eric Jang, Shixiang Gu, and Ben Poole. Categorical reparameterization with Gumbel-Softmax, 2017.
- Jaekyeom Kim, Minjung Kim, Dongyeon Woo, and Gunhee Kim. Drop-bottleneck: Learning discrete compressed representation for noise-robust exploration. *arXiv preprint arXiv:2103.12300*, 2021.
- Diederik P Kingma and Max Welling. Auto-encoding variational Bayes, 2014.
- Artemy Kolchinsky, Brendan D. Tracey, and David H. Wolpert. Nonlinear information bottleneck. *Entropy*, 21(12), 2019. ISSN 1099-4300. doi: 10.3390/e21121181. URL <https://www.mdpi.com/1099-4300/21/12/1181>.
- Chris J. Maddison, Andriy Mnih, and Yee Whye Teh. The concrete distribution: A continuous relaxation of discrete random variables, 2017.

- Aleksander Madry, Aleksandar Makelov, Ludwig Schmidt, Dimitris Tsipras, and Adrian Vladu. Towards deep learning models resistant to adversarial attacks, 2019.
- Hosam Mahmoud. *Pólya urn models*. Chapman and Hall/CRC, 2008.
- Ning Miao, Emile Mathieu, N. Siddharth, Yee Whye Teh, and Tom Rainforth. On incorporating inductive biases into VAEs, 2022.
- Norman Mu and Justin Gilmer. MNIST-C: A robustness benchmark for computer vision, 2019.
- Yaniv Ovadia, Emily Fertig, Jie Ren, Zachary Nado, David Sculley, Sebastian Nowozin, Joshua Dillon, Balaji Lakshminarayanan, and Jasper Snoek. Can you trust your model’s uncertainty? Evaluating predictive uncertainty under dataset shift. *Advances in Neural Information Processing Systems*, 32, 2019.
- Calyampudi Radhakrishna Rao. *Linear statistical inference and its applications*, volume 2. Wiley New York, 1973.
- Borja Rodríguez Gálvez, Ragnar Thobaben, and Mikael Skoglund. The convex information bottleneck Lagrangian. *Entropy*, 22(1):98, Jan. 2020. ISSN 1099-4300. doi: 10.3390/e22010098. URL <http://dx.doi.org/10.3390/e22010098>.
- Rachit Singh, Jeffrey Ling, and Finale Doshi-Velez. Structured variational autoencoders for the Beta–Bernoulli process. In *NIPS 2017 Workshop on Advances in Approximate Bayesian Inference*, 2017.
- Naftali Tishby and Noga Zaslavsky. Deep learning and the information bottleneck principle. In *2015 IEEE Information Theory Workshop (ITW)*, pages 1–5. IEEE, 2015.
- Naftali Tishby, Fernando C. Pereira, and William Bialek. The information bottleneck method, 2000.
- Jakub M Tomczak. *Deep Generative Modeling*. Springer Nature, 2022.
- Francesco Tonolini, Bjørn Sand Jensen, and Roderick Murray-Smith. Variational sparse coding. In *Uncertainty in Artificial Intelligence*, pages 690–700. PMLR, 2020.
- Florian Tramer, Nicholas Carlini, Wieland Brendel, and Aleksander Madry. On adaptive attacks to adversarial example defenses. *Advances in Neural Information Processing Systems*, 33:1633–1645, 2020.
- Florian Tramèr, Alexey Kurakin, Nicolas Papernot, Ian Goodfellow, Dan Boneh, and Patrick McDaniel. Ensemble adversarial training: Attacks and defenses, 2020.
- Serena Yeung, Anitha Kannan, Yann Dauphin, and Li Fei-Fei. Tackling over-pruning in variational autoencoders. *arXiv preprint arXiv:1706.03643*, 2017.
- Penglong Zhai and Shihua Zhang. Adversarial information bottleneck. *arXiv preprint arXiv:2103.00381*, 2021.

6 SUPPLEMENTARY MATERIALS

6.1 INFORMATION CURVE: SELECTION OF β

In the IB-Lagrangian, the Lagrange multiplier β controls the trade-off between two MI terms. By optimizing the IB-objective for different values of β we can explore the information curve, which is the plot of $(MI(X; Z), MI(Z; Y))$ in the 2-d plane. Figure S1 shows the information curve for the models selected for MNIST and F-MNIST for robustness studies in the main paper. For the fixed K VIB models trained for each dataset, the information curve is similar to Fig. S1. *Minimum necessary information* is a point in the information plane where $MI(X; Z) = MI(Z; Y) = H(Y)$, where entropy is denoted by $H(Y)$. For MNIST and F-MNIST, where the labels are deterministic given the images, the entropy $H(Y) = \log_2 10 \sim 3.32$. Therefore we pick the $\beta \sim 0.08$ for MNIST and $\beta \sim 0.06$ for F-MNIST, which gets us closest to the MNI. The points are circled in Fig. S1.

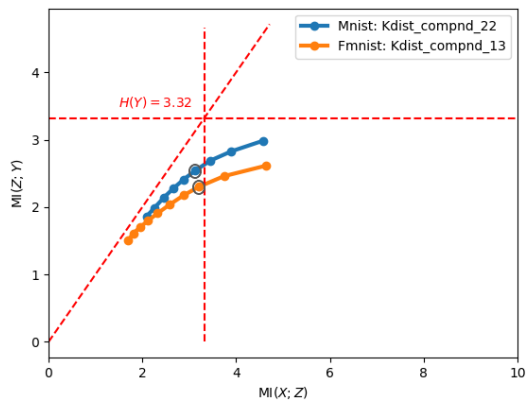


Figure S1: Information curve for compound (2,2) and (1,3) model on MNIST and F-MNIST, respectively.

6.2 SELECTION OF PRIOR PARAMETERS FOR CP-IB

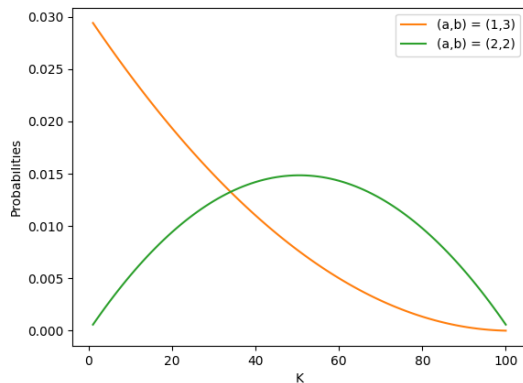


Figure S2: Plot of prior dimension probabilities for choices of (a, b) .

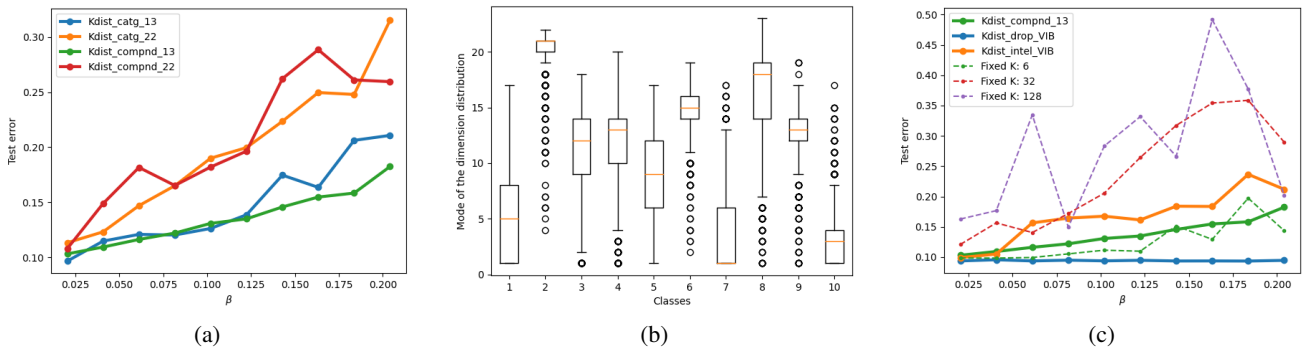


Figure S3: In-distribution results for F-MNIST.

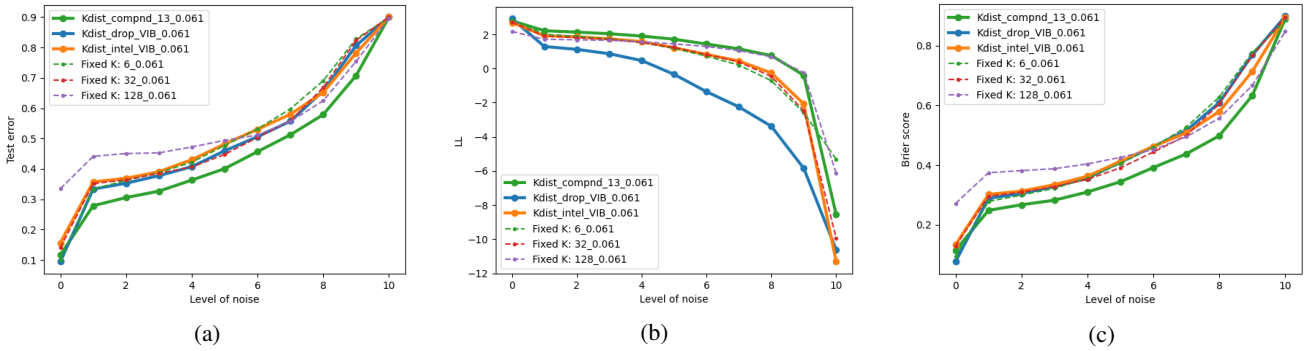


Figure S4: White-box attack results for F-MNIST. Plot of the test error, the log-likelihood, and the Brier score against level of noise added to the F-MNIST test dataset. We can observe that compound prior distribution with $(a, b) = (1, 3)$ (green solid line) performs best in most of the cases.

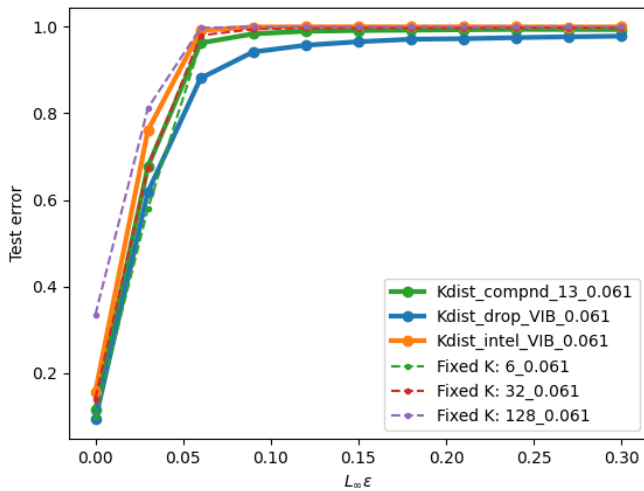


Figure S5: Plot of test error vs PGD L_∞ attack radius for 10 iterations on F-MNIST test set. The plot shows that Drop-VIB gives a lower test error than does our approach.